Chapter 4

Numerical solutions

The principal motivation for the **development and use of numerical models** for heat transport in subsurface environments was simulation of geothermal systems and heat storage in aquifers. In general, the development of numerical techniques was, to a large degree, anticipated by the development of models to simulate solute transport, starting in the 1970s. The **review** presented below concentrates on solutions of the advective and conductive heat transport problem in porous media, including both the saturated and unsaturated zones. Purely diffusive heat transport, a subject on which a vast number of contributions and models exist, is not considered here, since its numerical solution is formally identical to the solution of the diffusion equation (including the groundwater flow equation as a diffusion equation for pressure). Sometimes the solutions for pure heat conduction can be obtained from solutions for advection–dispersion–diffusion problems as special cases by setting the flow velocity equal to zero. The **heat transport problem** can be approximately solved in a **linearized form**, where temperature is influenced by flow, but flow is not influenced by temperature and density and hydraulic conductivity are assumed constant. This one-way coupling of flow and heat transport is the general assumption of authors. Alternatively, a **fully two-way coupled solution** is feasible where an iteration of the nonlinear system becomes necessary.

Mercer et al. (1982) presented a review on current simulation techniques for thermal energy storage in aquifers. Mercer et al. (1975) developed a transient two-dimensional model for the simulation of areal (horizontal) water flow and heat transport in a saturated aquifer, using the Galerkin finite element technique. Water viscosity and water density were taken as temperature dependent. They used the model to evaluate the hot-water geothermal system Wairakei (New Zealand), without taking into account phase-change processes. Their results were in general correspondence with the field data. Werner and Kley (1977) developed a three-dimensional finite difference model using cylindrical coordinates for the investigation of heat storage in aquifers. Radial flow velocity was assumed and dispersion

effects were taken into account. They were able to approximately simulate a hydrothermal field experiment near Krefeld (Germany).

The **Lawrence Berkeley Laboratory** (Lippmann et al. 1977) developed the code CCC, which stands for conduction, convection, and consolidation, to simulate the coupled heat and momentum transport in one-, two-, and three-dimensional heterogeneous, anisotropic, nonisothermal porous media. Tsang et al. (1981) used this code to simulate the Auburn University field experiments (United States). They modeled two cycles of seasonal aquifer thermal energy storage (ATES). Simulated production temperatures and energy recovery factors agreed well with the field data.

Doughty et al. (1982) presented a dimensionless parameter approach to predict the thermal behavior of an ATES system. The analysis was restricted to radial flow in a horizontal aquifer confined by impermeable layers neglecting buoyancy effects. The heat transport equation was numerically integrated using an explicit finite difference approach.

Sauty et al. (1982) presented a theoretical study on the thermal behavior of a hot water storage system in an aquifer using a single well. They developed an axially symmetrical model, solved it applying a finite difference scheme, and checked it against analytical solutions. Buoyancy effects were neglected. The model was then used to evaluate the well temperature during production periods for symmetrical cycles (production volume and flow rate equal to injection volume and flow rate). They used both a fully implicit conductive scheme and an upstream explicit advective scheme. From the results, they deduced type curves for sets of dimensionless parameters.

Wiberg (1983) analyzed transient heat storage in an aquifer using the finite element method. His basic theory included nonlinear thermal physical properties and boundary conditions. Numerical simulations are shown for a purely conductive case with heat storage and a one-dimensional conductive–advective heat transport problem with a nonlinear decay term. Xue et al. (1990) used a three-dimensional alternating-direction implicit scheme to solve the heat transport equation. The flow was assumed as radial and heat transport included heat dispersion. The model was successfully used to investigate aquifer thermal heat storage in groundwater in China.

Merheb (1984) formulated a horizontal two-layer groundwater flow model and a corresponding heat transport model with heat exchange between layers and soil surface using a finite difference technique. The flow and the heat transport models were implemented in an uncoupled, sequential manner. He applied the model for the Strasbourg region (France).

Molson et al. (1992) formulated a three-dimensional finite element model for simulating coupled density-dependent groundwater flow and heat transport in aquifers. The heat transport solution is based on a finite element time integration, which generates a symmetrical coefficient matrix. The thermal transport model was successfully checked against the results of the Borden (Canada) thermal injection field experiment. Dwyer and Eckstein

(1987) formulated a two-dimensional, horizontal, Galerkin finite element model for a feasibility study of ATES coupled with a heat pump. The flow and the heat transport models were applied in an uncoupled, sequential manner. In heat transport, advection and mechanical dispersion were taken into account.

Sun and Carrington (1995) developed a so-called implicit correction scheme for advection-dominated heat transfer in porous media with strong temperature gradient. The scheme allows relatively coarse grid size for the numerical discretization. Chevalier and Banton (1999) used the random walk method to study heat transfer problems in porous media with a radial flow field. Buoyancy effects were disregarded and none of the physical properties were dependent on the temperature. They checked the model against analytical and numerical solutions. Kohl and Hopkirk (1995) presented the simulation code FRACTure for forced water flow in fractured rocks. Hydrodynamics were coupled to rock mechanics but not to heat transport. They applied the code to hot dry rock sites. Signorelli et al. (2007) used this code for a numerical evaluation of thermal response tests. Hecht-Méndez et al. (2010) used MT3DMS (Zheng and Wang 1999) to simulate heat transport in closed geothermal systems, assuming that buoyancy effects and temperature dependency of water viscosity are negligible. They compared their results with those of analytical solutions and numerical solutions using SEAWAT (Langevin et al. 2008) and found good agreement.

Diersch and Kolditz (1998) analyzed double-diffusion and buoyancy driven free-convection processes using the code FEFLOW (Diersch 1996).

Chiasson et al. (2000) numerically investigated the effects of groundwater flow on closed-loop ground-source heat pump systems and postulated that heat advection can significantly enhance heat transfer from and to borehole heat exchangers (BHEs). Similar conclusions were drawn by Fan et al. (2007). An initial assessment of the importance of advection can be obtained by an examination of the thermal Peclet number (Chiasson et al. 2000).

Ferguson (2007) examined the effect of heterogeneities on heat transport by stochastic modeling, including dispersion effects using geostatistics of aquifers. His results indicate that there is considerable uncertainty in the distribution of heat associated with the injection of warm water into an aquifer. Advective–conductive heat transport models were created using METRA, which is a submodule of the code MULTIFLOW (Painter and Seth 2003). METRA is an integrated finite difference code capable of simulating variable-density fluid flow and heat flow. Hidalgo et al. (2009) performed a Monte Carlo analysis of steady-state advective–conductive heat transfer in heterogeneous aquifers using a finite element code.

Graf and Therrien (2007) formulated a model for coupled fluid flow, heat, and single-species reactive mass transport with variable fluid density and viscosity in fractured porous media. The effects were incorporated in

the code HydroGeoSphere. Brookfield et al. (2009) performed a numerical study on thermal transport modeling in a fully integrated surface–subsurface framework using this code.

Engeler et al. (2011) investigated heat transport in an aquifer with strong river–aquifer interaction. They used the code SPRING (delta-h 2012), which uses three-dimensional finite elements and allows temperature dependence of the flow parameters. They showed that better agreement with measured temperature data is obtained if the temperature dependence of the leakage coefficient (via the temperature dependence of viscosity) is taken into account in the modeling.

Several authors have also investigated heat transport in unsaturated porous media. Sophocleous (1979) formulated an implicit vertical finite difference model for the analysis of coupled nonlinear water and heat transport under saturated and unsaturated conditions. He used and extended the Philip and de Vries (1957) formulation of coupled nonisothermal flow of water, vapor, and heat (Parlange et al. 1998). Yeh and Luxmore (1983) presented a multidimensional model for moisture and heat transport in unsaturated porous media using the so-called integrated compartment method, which is an extension of the integrated finite difference method. Again, the Philip and de Vries (1957) nonisothermal equations were used for simultaneous moisture and heat transport. Sidiropoulos and Tzimopoulos (1983) performed a sensitivity analysis of coupled water and heat transfer in porous media. For their case, they found that phase-change effects could be neglected. Birkholzer and Tsang (2000) used the code TOUGH2 (Wu et al. 1996) for the modeling of the coupled thermohydraulic processes in a large-scale underground heater test in partially saturated fractured tuff.

Al-Khoury (2012), Al-Khoury and Bonnier (2006), and Al-Khoury et al. (2005, 2010) presented computationally efficient finite element tools for the analysis of three-dimensional steady-state and transient heat flow in geothermal systems. They assumed that temperature has no influence on groundwater flow. They formulated one-dimensional heat pipe finite elements, which are capable of simulating pseudo-three-dimensional heat flow in a vertical BHE consisting of pipe-in, pipe-out, and grout material. Three-dimensional finite elements for saturated aquifers were formulated, which can be in contact with heat pipe finite elements. Their method was extended by Bauer et al. (2011) and Diersch et al. (2011a,b) and incorporated in the software FEFLOW (DHI-WASY 2010).

Glück (2011) developed engineering software for the numerical simulation of underground heat exchangers. Steady-state and transient axially symmetrical temperature fields due to heat conduction are calculated using the finite volume method. Thermal processes within the BHE with inflow and outflow tubes (single- and double-U-tube configuration) embedded in grouting material are restricted to quasi-steady-state conditions and are evaluated using the concept of heat transfer coefficients. By

evaluating an effective radius of a single device, regular fields of BHEs are approximated.

Lazzari et al. (2010) investigated the long-term performance of BHE fields with negligible groundwater movement by finite elements using the software package COMSOL. Lee and Lam (2008) performed computer simulations for BHE systems using the finite difference approach. Outside the borehole, heat transport is restricted to heat conduction. Inside the borehole, flow in the tubes is incorporated. Fujimitsu et al. (2010) numerically evaluated the environmental impact caused by a ground-coupled heat pump system using the FEFLOW software. Park et al. (2012) investigated the heat transfer of helical BHEs experimentally, analytically, and numerically. Park et al. (2013) numerically modeled precast, high strength concrete energy piles. Jalaluddin and Miyara (2012) numerically investigated the performance of several types of vertical BHEs in continuous and discontinuous operation modes with the software FLUENT.

Laloui et al. (2006) formulated a coupled displacement, pore water pressure, temperature finite element model for heat exchanger piles. The model was able to reproduce in situ experimental observations.

Deng et al. (2005) suggested and tested a simplified numerical model for the simulation of standing column well ground heat exchangers. Woods and Ortega (2011) numerically investigated the thermal response of a line of standing column wells and compared these results with analytical models.

Kim et al. (2010) numerically investigated the performance of ATES systems in confined aquifers (open systems). They formulated a three-dimensional aquifer flow and heat transport model with finite elements, assuming constant water density and viscosity, using COMSOL. They concluded that the thermal interference of an ATES system (affecting primarily the system performance) depends on the distance between the two boreholes, the hydraulic conductivity of the aquifer, and the production/injection rate. The thermal interaction of pumping and injecting well groups with absent regional groundwater flow was numerically investigated by Gao et al. (2013). They assumed that material properties do not depend on temperature.

4.1 TWO-DIMENSIONAL HORIZONTAL NUMERICAL SOLUTIONS

Two-dimensional numerical solutions are mainly discussed here with respect to their application concerning **open thermal systems**, that is, systems with water abstraction and reinfiltration after temperature increase or decrease by ΔT. The **vertically integrated, two-dimensional heat transport equation for shallow regional aquifers** focuses on the saturated part, as recalled here:

$$\frac{\partial T}{\partial t} = \nabla \cdot (\mathbf{D}_t \nabla T) - \frac{C_w}{C_m} \nabla \cdot (\mathbf{q} T) + \frac{P_t}{m C_m} + \frac{J_{vert,bot}}{m C_m} + \frac{J_{vert,top}}{m C_m} \tag{4.1}$$

The variable $T(\mathbf{x}, t)$ is the mean temperature in a vertical profile at location $\mathbf{x}$ and time t. Vertical heat flow from below (geothermal heat flux), $J_{vert,bot}(\mathbf{x}, t)$, and vertical advective and diffusive heat transport from soil surface to aquifer, $J_{vert,top}(\mathbf{x}, t)$, are taken into account through source/sink terms. While the former can be expressed and inserted directly, the latter can be treated in a different manner. In the application of the two-dimensional heat transport equation, it is often assumed that the coupling of flow and transport via density can be neglected.

One possibility consists of inserting the **linear approximation for the vertical heat flux** $J_{vert,top}(\mathbf{x}, t)$ into the heat transport equation:

$$\frac{\partial T}{\partial t} = \nabla \cdot (\mathbf{D}_t \nabla T) - \frac{C_w}{C_m} \nabla \cdot (\mathbf{q} T) + \frac{P_t}{m C_m} + \frac{J_{vert,bot}}{m C_m} + \frac{\lambda_{vert} \cdot (T_{surface} - T)}{m C_m \cdot (f + m/2)} + \frac{N C_w T_{surface}}{m C_m} \tag{4.2}$$

Equation 4.2 is expressed here as the transient balance equation. However, we have to keep in mind that the transient behavior is not fully considered, or only in a rudimentary way, for the linear flux terms from soil surface to groundwater. This disadvantage is avoided for l**ong-term, steady-state flow and heat transport** according to

$$\nabla \cdot (\mathbf{D}_t \nabla T) - \frac{C_w}{C_m} \nabla \cdot (\mathbf{q} T) + \frac{P_t}{m C_m} + \frac{J_{vert,bot}}{m C_m} + \frac{\lambda_{vert} \cdot (T_{surface} - T)}{m C_m \cdot (f + m/2)} + \frac{N C_w \cdot (T_{surface} - T_0)}{m C_m} = 0 \tag{4.3}$$

Furthermore, if we adopt the considerations pointed out in Chapter 2.1.3.1 to formulate the equation in terms of **temperature differences** $\Delta T(\mathbf{x}) = T(\mathbf{x}) - T_{surface}(\mathbf{x})$ and to choose $T_0 = T_{surface}$ assuming **constant surface temperature,** Equation 4.3 reduces to

$$\nabla \cdot (\mathbf{D}_t \nabla T) - \frac{C_w}{C_m} \nabla \cdot (\mathbf{q} T) + \frac{P_t}{m C_m} + \frac{J_{vert,bot}}{m C_m} + \frac{\lambda_{vert} \cdot (T_{surface} - T)}{m C_m \cdot (f + m/2)} = 0 \tag{4.4}$$

The equation formally corresponds to the steady-state solute transport equation with first-order decay.

A main contribution to the heat production term P_t is the heat flux from **large warm basements of constructions**. The vertical contribution can be approximately expressed according to Equation 2.125 by

$$J_{\text{cond\_basement}} = A_{\text{basement}}\lambda_{\text{vert}}\frac{T_{\text{basement}} - T_{\text{gw}}}{\left(f+\frac{m}{2}\right)_{\text{basement}}} = A_{\text{basement}}\lambda_{\text{vert}}\frac{(T_{\text{basement}} - T_0) - (T_{\text{gw}} - T_0)}{\left(f+\frac{m}{2}\right)_{\text{basement}}}$$

$$= A_{\text{basement}}\lambda_{\text{vert}}\frac{(T_{\text{basement}} - T_0) - T_{\text{rel}}}{\left(f+\frac{m}{2}\right)_{\text{basement}}} \tag{4.5}$$

Therefore, the heat flux consists of a first-order part in $T_{\text{rel}} = T_{\text{gw}} - T_0$ and a constant heat flux. The latter represents a heat-loading rate.

Another interesting possibility consists of **coupling the two-dimensional heat transport equation for the (saturated) regional aquifer with the one-dimensional vertical heat-flow between soil surface and aquifer**. In water flow problems, this coupling has been realized in HYDRUS-1D-MODFLOW (Seo et al. 2007). It can be achieved, in principle, by adding vertical columns on top of each finite difference cell or finite element. In practice, however, areas of identical parameters and conditions are defined within the solution domain D in order to reduce the computational effort.

In the case of **confined aquifers**, the **vertical heat flux** $J_{\text{vert,top}}(\mathbf{x}, t)$ at the top of the aquifer is described by the heat transport equation in solids, according to Equation 2.101, here without production term:

$$\frac{\partial T}{\partial t} = \frac{\partial}{\partial z}\left[D_t\frac{\partial T}{\partial z}\right] \tag{4.6}$$

Coupling of the two models requires the continuity of temperature and the continuity of the heat flux.

For **unconfined aquifers, the vertical heat balance equation**, that is,

$$\frac{\partial T}{\partial t} = \frac{\partial}{\partial z}\left[(D_{\text{t,diff}} + D_{\text{t,disp,L}})\frac{\partial}{\partial z}T\right] - \frac{C_w}{C_m}\frac{\partial}{\partial z}(q_z T) \tag{4.7}$$

has to be coupled with the water flow equation, that is, the **vertical Richards equation**:

$$\phi\frac{\partial S_w}{\partial t} = \frac{\partial}{\partial z}\left(K_w(S_w)\frac{\partial}{\partial z}\left(z + \frac{p_w}{\rho_w g}\right)\right) \tag{4.8}$$

Coupling of the models now requires the continuity of temperature and water, as well as heat fluxes at the interface between the two regions. With this procedure, the computational effort can be reduced considerably compared to a three-dimensional saturated–unsaturated model. In principle, the coupling with vertical soil columns can also be undertaken in connection with a multilayer flow and heat transport model.

4.1.1 Analogy with solute transport models

Obviously, one may **utilize any existing solute transport code** for heat transport as well, if one establishes the analogy between both models in a consistent way. The principle is shown using the example of Equation 4.4. A comparison with the **steady-state solute transport equation**, that is,

$$\nabla \cdot (\mathbf{D}_h \nabla c) - \frac{1}{\phi} \nabla \cdot (\mathbf{q} c) + \frac{P_c}{m\phi} - \lambda_c c = 0 \tag{4.9}$$

yields the following correspondence between the parameter

Solute transport	*Heat transport*
Solute concentration $c \geq 0$	Temperature $T_{rel} \geq 0$
Hydrodynamic dispersion tensor $\mathbf{D}_h$	Thermal dispersion tensor $\mathbf{D}_h$
Molecular diffusion coefficient D_{mol}	Thermal diffusion coefficient D_t
Macrodispersivities α_L, α_T	Macrodispersivities β_L, β_T
Inverse porosity $1/\phi_c$	Thermal capacity ratio C_w/C_m
Source/sink term $P_c/(\phi m)$	Thermal source/sink $P_t/(C_m\, m)$
Decay coefficient λ_c	Thermal flux coefficient $\lambda_{vert}/(C_m m(f + m/2))$

Therefore, in order to simulate heat transport using a solute transport code, the parameters have to be defined as follows. In the solute transport code, **equivalent porosity** is

$$\phi_c = \frac{C_m}{C_w} \tag{4.10}$$

The **equivalent solute mass production** term is

$$P_c = \frac{P_t \phi}{C_m} \tag{4.11}$$

and the **equivalent decay coefficient** is

$$\lambda_c = \frac{\lambda_{vert}}{C_m m \cdot \left(f + \frac{m}{2} \right)} \tag{4.12}$$

Consequently, the **heat injection** rate $J_t = QC_w\Delta T$ translates into the analogous solute mass flux $J_c = Q\Delta c$. Note that since solute concentrations have to be positive, with $c \geq 0$, the relative temperature has to be positive as well, with $T_{rel} \geq 0$.

The **assumption of constant mean surface temperature** represents a simplification of the complex processes at the soil surface (see Chapter 1). In fact, it cannot be excluded that an increase or decrease in groundwater temperature could also affect the temperature at the soil surface. Such a situation could arise, for example, for aquifers with very small depth to groundwater.

We are not aware that codes exist that solve Equation 4.4 or its transient form. However, several codes exist that solve the **solute transport equation with first-order decay**, like MT3D (Zheng 1990), MT3DMS (Zheng and Wang 1999), HydroGeoSphere (Graf and Therrien 2007; Raymond et al. 2011), FEFLOW (DHI-WASY 2010), SPRING (delta-h 2012), and others. They can be used as analogs in order to solve thermal processes in two-dimensional aquifers. In any case, a simulation of thermal or solute transport requires the simulation of the water flow field beforehand.

4.1.2 Analysis of steady-state open system in rectangular aquifer

The procedure for simulating heat transport using a solute transport code is illustrated for the **example** of a simple rectangular confined aquifer of size 2000 m × 1000 m, of thickness m = 12 m, and with hydraulic conductivity K_w = 0.002 m s^{-1} (Figure 4.1). No areal recharge occurs. Piezometric head is

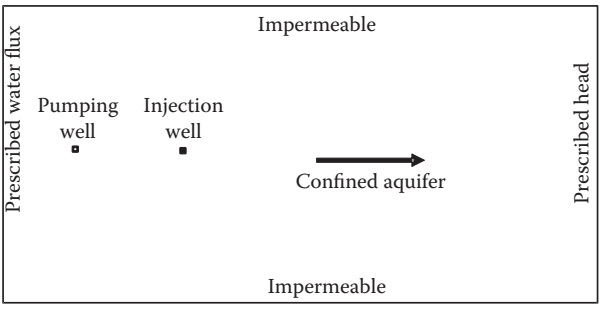

Figure 4.1 Illustrative example of two-dimensional aquifer: situation and hydraulic boundary conditions.

specified at the western boundary with h_w = 12 m. At the eastern boundary, the water inflow rate is specified with a total flow rate of Q_{inflow} = 0.036 m^3 s^{-1}. Without wells, this corresponds to a flow gradient of 0.0015. Impermeable boundaries are present at the northern and southern boundaries. Thermal use is planned for an open system with extraction well, heat pump, and infiltration well. The pumping rate is Q_w = 1000 m^3 day^{-1}. Since thermal use occurs in the winter season only, Q_w corresponds to a yearly average value. The distance between extraction and infiltration well is chosen in order to avoid hydraulic short-circuiting for the actual pumping rate in the winter season. The steady-state flow field is shown in Figure 4.2 with results from particle tracking indicating flow lines. The equivalent porosity value is ϕ_c = 0.571, using $C_m = 2.4 \times 10^6$ W m^{-3} K^{-1}. Markers on the particle tracks are shown in yearly intervals based on the velocity u_t of the thermal front.

The longitudinal thermal macrodispersivity is chosen as β_L = 10 m and the transversal macrodispersivity as β_T = 1 m. The size of the finite difference cells is 10 m. Boundary conditions are prescribed temperature T_{rel} = 0 at the eastern boundary, impermeable northern and southern boundaries, and the transmission boundary type (Chapter 2.1.2.5) for the western boundary. The latter is approximated by setting longitudinal dispersivity to zero along the outflow boundary. Water is pumped at the abstraction well. A heat pump lowers the temperature by 3 K. This is realized by setting a positive source concentration of c_{well} = 3.0. The equivalent decay coefficient is calculated using Equation 4.12, with λ_{vert} = 2.0 W m^{-1} K^{-1} and f = 6 m, which yields $\lambda_c = 5.787 \times 10^{-9}$ s^{-1}. The transport module was run for 20 years in order to approach steady-state thermal conditions. The thermal plume after 20 years of infiltration of cold water is shown in Figure 4.3. Note that this type of steady-state (time-averaged) analysis does not take into account the dynamics caused by seasonally varying pumping and infiltration rates. The

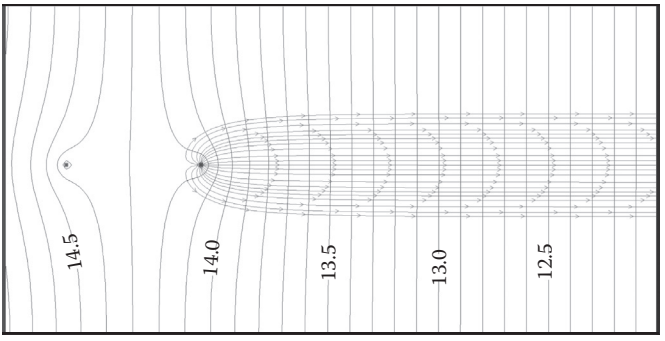

Figure 4.2 Illustrative example of two-dimensional aquifer: steady-state flow field with step in piezometric head Δh_w = 0.1 m. Particle tracks starting at infiltration well. Particle markers are introduced with increment Δt = 1 year (with respect to thermal velocity).

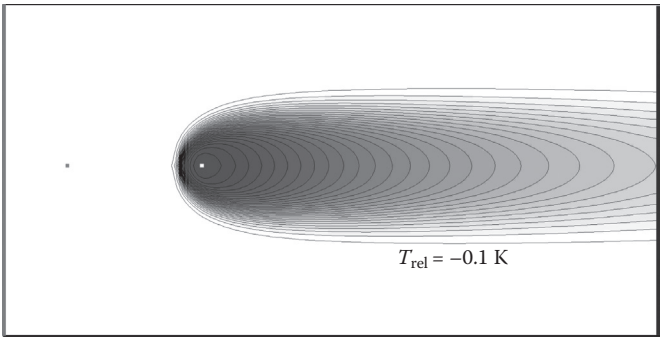

Figure 4.3 Illustrative example of two-dimensional aquifer: calculated thermal plume due to infiltration of cold water with ΔT = 3 K, after 20 years. Temperature increment is 0.1 K.

latter would cause more lateral spreading of the thermal plume during the cold season and, therefore, also in the long run. Furthermore, it is important to realize that macrodispersion effects are usually overestimated close to the source, that is, the infiltration well. This has to do with the scale-effect of macrodispersivity as described in Chapter 2.1.2.3.

The example was calculated using standard MODFLOW-96 (USGS 2012) and MT3DMS (Zheng and Wang 1999), which are both incorporated in the code PMWIN (Chiang and Kinzelbach 2005). Transport was simulated using an upstream finite difference scheme with discretization $\Delta x = \Delta y = 10$ m and a time step corresponding to a Courant number of 0.75 (see Equation 4.32). The grid Peclet number (see Equation 4.30) was 2.

4.1.2.1 Scaled solution for open system in rectangular aquifer

For the simple rectangular layout of the illustrative example, the procedure can be extended by **scaling**. By introducing a **length scale** L, any length can be scaled such as $x' = x/L$ or $h'_w = h_w/L$. The **steady-state scaled form of the two-dimensional flow equation** 2.38 is

$$\nabla'^2 h'_w + \frac{NL}{K_w m} = 0 \tag{4.13}$$

where ∇'^2 is the Laplace operator, in scaled form. We may choose the length scale as $L = Q/(mq_0)$ using the pumping and infiltration rate Q and the specific inflow rate q_0. Note that in this case, L is the recharge width of the flow toward the well.

Using the specified inflow rate q_0 to scale the water fluxes, and introducing a temperature scale Θ, the **scaled steady-state heat transport equation** without P_t and $J_{vert,bot}$ is

$$\frac{\beta_L}{L}\nabla'\cdot(\mathbf{D}'_t\nabla T'_{rel})-\nabla'\cdot(\mathbf{q}'T'_{rel})+\frac{\lambda_{vert}T'_{rel}Q}{(f+m/2)m^2q_0^2C_w}=0 \tag{4.14}$$

assuming that macrodispersion is dominant compared to thermal diffusion. The temperature scale may be chosen as $\Theta = \Delta T$. The **decay term** can be written as $\lambda'_{vert}T'_{rel}$ with the dimensionless decay coefficient λ'_{vert}:

$$\lambda'_{vert}=\frac{\lambda_{vert}Q}{(f+m/2)m^2q_0^2C_w} \tag{4.15}$$

A **time scale** τ can be obtained by setting $\tau = L/u_t = LC_m/(C_w q_0)$.

The **scaled temperature field is evaluated numerically** and analyzed for the scaled temperature profile along the streamline through the infiltration well. For $\lambda'_{vert} = 0.01$, 0.1, and 1, the dimensionless longitudinal dispersivity $\beta'_L = \beta_L/L = 0.02$ (which represents a small value), and the dispersivity ratio $\beta'_T/\beta'_L = 0.1$, the scaled temperature profile is shown in Figure 4.4. For $\beta_L = 0.2$ (representing a medium value) and again $\beta'_T/\beta'_L = 0.1$, it is shown in Figure 4.5. Obviously, there is quite some impact of dispersion on the shape of the plume. We can state that the shape is mainly governed by decay. Again, one has to be aware that dispersion effects are overestimated close to the infiltration well.

The numerical scaling analysis was again performed using standard MODFLOW-96 (USGS 2012) and MT3DMS (Zheng and Wang 1999), which are both incorporated in the code PMWIN (Chiang and Kinzelbach 2005).

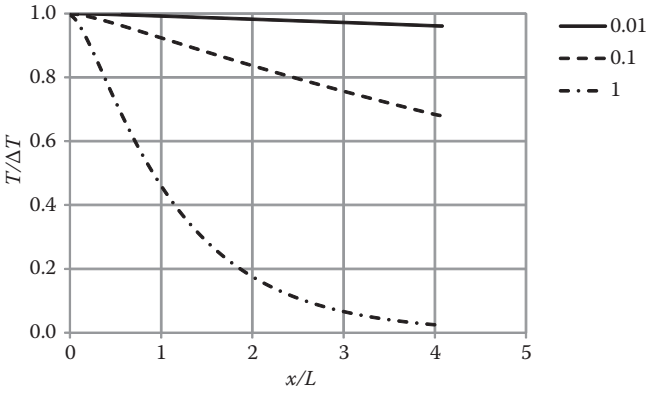

Figure 4.4 Scaled steady-state temperature profile downstream of the infiltration well in simple two-dimensional aquifer for dimensionless decay coefficients $\lambda'_{vert} = 0.01$, 0.1, 1 and $\beta'_L = 0.2$, $\beta'_T = 0.02$.

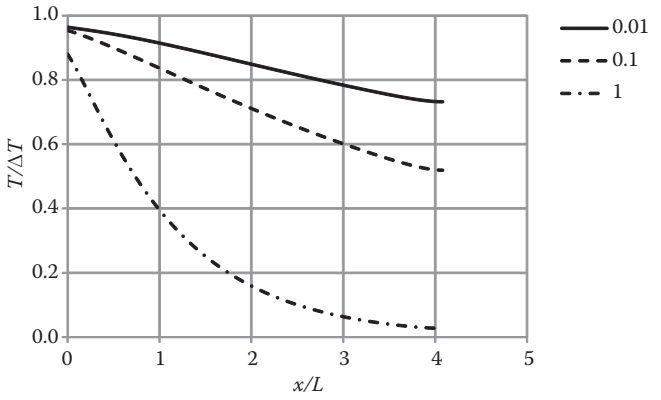

Figure 4.5 Scaled steady-state temperature profile downstream of the infiltration well in simple two-dimensional aquifer for dimensionless decay coefficients $\lambda'_{vert} = 0.01$, 0.1, 1 and $\beta'_L = 0.2$, $\beta'_T = 0.02$.

Transport was simulated using an upstream finite difference scheme with discretization $\Delta x' = \Delta y' = 0.02$ and a time step corresponding to a Courant number of 0.75 (see Equation 4.32). Results are shown for the dimensionless time $t' = 10$.

4.2 MULTIDIMENSIONAL NUMERICAL SOLUTIONS

Solution techniques are briefly discussed with respect to the **solution of the heat transport equation** 2.92 including heat advection:

$$\frac{\partial T}{\partial t} = \nabla \cdot [\mathbf{D}_t \nabla T] - \frac{C_w}{C_m} \nabla \cdot (\mathbf{q}T) + \frac{P_t}{C_m} \tag{4.16}$$

Frequently used **numerical solution methods** can be classified as follows:

- Finite difference method
- Finite element method
- Finite volume method
- Method of characteristics
- Random walk method

Note that in each group, various submethods and techniques have been formulated. In the following, we concentrate on basic ideas of the methods.

4.2.1 Principles of the finite difference method for heat transport

For the presentation of the principles, we prefer to start from the **energy balance equation**:

$$C_m \frac{\partial T}{\partial t} = \nabla \cdot \left[(\lambda_m + C_w \mathbf{D}_{t,disp}) \nabla T \right] - C_w \nabla \cdot (\mathbf{q} T) + P_t \tag{4.17}$$

The basic procedure of the **finite difference method** can be stated as follows: The solution domain D is **discretized into prismatic cells**. In the case of one- and two-dimensional problems, the shape reduces to linear and rectangular cells. Numbering of the cells is chosen according to three-dimensional matrices with layer, row, and column indices i, j, k. The cell size does not need to be constant. However, neighboring cells should still have similar size (change less than a factor of 2) for numerical reasons.

For each cell, the mean temperature $T_{ijk}(t)$ is either unknown (and to be calculated) or known (prescribed temperature). This temperature corresponds to the average value within the cells. The temperature $T_{ijk}(t)$ is assigned to the cell center.

For each cell (i, j, k), the **physical heat balance** is expressed over all surfaces of the cell using unknown temperatures $T_{ijk}(t + \Delta t)$ within the cells, given known temperatures in each cell, where Δt is the time step. The advective, diffusive, and dispersive heat fluxes are expressed by linear approximations, using the cell center temperatures from the neighboring cells. The **rate of change of the energy within the cell** is expressed using the time step Δt and the temperature difference $T_{ijk}(t + \Delta t) - T_{ijk}(t)$.

Boundary conditions (like prescribed temperature or prescribed heat flux) are directly considered in the corresponding balance equations for the cells. The resulting **equation system** is linear in the unknown temperatures at time $(t + \Delta t)$. After obtaining the solution, the new temperatures $T_{ijk}(t + \Delta t)$ in the cells are the **initial conditions for a new time step**.

The **advective heat flux** in x-direction into the cell (i, j, k) (Figure 4.6) can be expressed as follows:

$$\begin{aligned} J_{x,i,j,k,adv}(t^*) = {} & q_{x,i-\frac{1}{2},j,k}(t^*) C_w T_{i-\frac{1}{2},j,k}(t^*) \Delta y \Delta z \\ & - q_{x,i+\frac{1}{2},j,k}(t^*) C_w T_{i+\frac{1}{2},j,k}(t^*) \Delta y \Delta z \end{aligned} \tag{4.18}$$

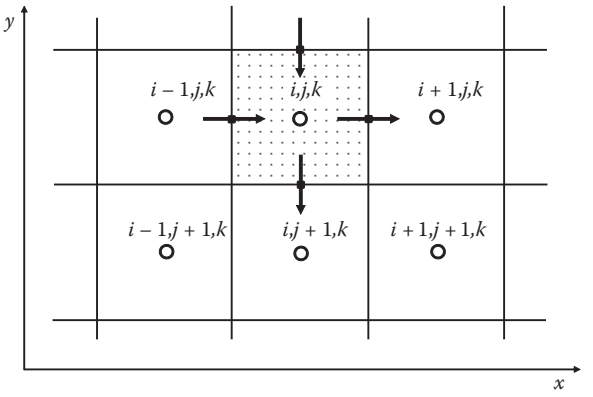

Figure 4.6 Finite difference grid with cell *i,j,k*.

The time t^*, at which the fluxes are determined, has to be specified. The index $i - 1/2$ and $i + 1/2$, respectively, denote the values at the interfaces between the cells. This formulation presumes therefore that the central value between adjacent cells is taken (central scheme). A (first-order) **upwind scheme** gives more weight to the upstream cell. This can increase stability of advective transport simulation, but may increase numerical diffusion (see Pe-criterion below). If these cell indices are *in* (*i*, or *i*–1) and *out* (*i* or *i*–1), respectively, depending on the water flow direction, the heat flux can be written as

$$J_{x,i,j,k,\mathrm{adv}}(t^*) = q_{x,i-\frac{1}{2},j,k}(t^*)C_{\mathrm{w}}T_{\mathrm{in},j,k}(t^*)\Delta y\Delta z - q_{x,i+\frac{1}{2},j,k}(t^*)C_{\mathrm{w}}T_{\mathrm{out},j,k}(t^*)\Delta y\Delta z \tag{4.19}$$

The **conductive heat flux** into the cell is expressed as

$$J_{x,i,j,k,\mathrm{diff}}(t^*) = \frac{\lambda_{x,i-\frac{1}{2},j,k}\cdot\left(T_{i,j,k}(t^*) - T_{i-1,j,k}(t^*)\right)}{\Delta x}\Delta y\Delta z - \frac{\lambda_{x,i-\frac{1}{2},j,k}\cdot\left(T_{i+1,j,k}(t^*) - T_{i,j,k}(t^*)\right)}{\Delta x}\Delta y\Delta z \tag{4.20}$$

In a corresponding manner, the **dispersive flux** in x-direction caused by a temperature gradient in x-direction is

$$J_{x,\mathrm{disp},xx}(t^*) = \frac{D_{xx,i-\frac{1}{2},j,k} \cdot \left(T_{i,j,k}(t^*) - T_{i-1,j,k}(t^*)\right)}{\Delta x} \Delta y \Delta z - \frac{D_{xx,i-\frac{1}{2},j,k} \cdot \left(T_{i+1,j,k}(t^*) - T_{i,j,k}(t^*)\right)}{\Delta x} \Delta y \Delta z \quad (4.21)$$

The **dispersive flux in x-direction caused by a temperature gradient in y-direction**, using interpolation of the gradient to the center of the exchanging interface, is

$$J_{x,\mathrm{disp},xy}(t^*) = \frac{C_\mathrm{w} D_{xx,i-\frac{1}{2},j,k} \cdot \left(T_{i-1,j-1,k}(t^*) - T_{i-1,j+1,k}(t^*) + T_{i,j-1,k}(t^*) - T_{i,j+1,k}(t^*)\right)}{4\Delta y} \Delta y \Delta z - \frac{D_{xx,i-\frac{1}{2},j,k} \cdot \left(T_{i+1,j,k}(t^*) - T_{i,j,k}(t^*)\right)}{\Delta x} \Delta y \Delta z \quad (4.22)$$

In a similar manner, all dispersive fluxes into the cell can be expressed. In order to express the dispersive fluxes in a symmetric way, a total of 26 neighboring cells are needed in three dimensions.

Finally, the **heat storage** in the cell (i, j, k) is

$$\frac{C_\mathrm{m} \cdot \left(T_{i,j,k}(t + \Delta t) - T_{i,j,k}(t)\right) \Delta x \Delta y \Delta z}{\Delta t} = \sum_{i=x,y,z} \left(J_{i,\mathrm{adv}}(t^*) + J_{i,\mathrm{diff}}(t^*) + \sum_{j=x,j,z} J_{i,\mathrm{disp\_}ij}(t^*) \right) + P_{\mathrm{t},i,j,k}(t^*) \quad (4.23)$$

Still, the time t^*, at which the fluxes are determined, remains to be specified.

If all fluxes are evaluated at the old time level, that is, $t^* = t$, one obtains an **explicit scheme**. This formulation is attractive since all fluxes can be evaluated directly without the need to solve an equation system. The only unknown is the temperature $T_{ijk}(t + \Delta t)$ appearing in the storage term, which can be computed in an explicit manner. However, the time step needs to be small enough in order to guarantee stability. It is required that the diffusive and dispersive thermal fluxes into any cell are smaller than the rate of change of energy within the cell:

$$2 \cdot (\lambda_m + C_w D_{t,disp,L}) \frac{T}{\Delta s} \leq \frac{C_m T \Delta s}{\Delta t} \tag{4.24}$$

This leads to the **von Neumann criterion for the time step** Δt of explicit schemes, which states

$$\Delta t \leq \frac{C_m \Delta s^2}{2 \cdot (\lambda_m + C_w D_{t,disp,L})} = \frac{\Delta s^2}{2 D_t} \tag{4.25}$$

where Δs is the **spatial discretization** (Δx, or Δy, or Δz).

Using $t^* = t + \Delta t$ yields a fully **implicit scheme**, while for a **Crank–Nicolson scheme**, $T(t^*) = 0.5 \cdot (T(t + \Delta t) + T(t))$ (time-centered) is applied (which also leads to implicit equations). Very often in available codes, the difference scheme is an input parameter and has to be selected: upwind or central in space, and explicit, implicit, or centered in time. For the implicit and the time-centered schemes, a **linear equation system** is obtained, of the form

$$\sum_{j=1}^{n} A_{ij} T_j = b_i; \quad i = 1, ..., n \tag{4.26}$$

where A_{ij} is a term of the coefficient matrix, T_j is a component of an unknown vector of the temperature in the cells, b_i is a constant term, and n is the number of cells. The resulting **matrix** [A] is sparse, since only the neighboring cells are involved in the balance equations. In contrast to the flow equations, in general, matrix [A] is **not symmetric**. The reason lies in the advective terms. Adapted numerical techniques, like the biconjugate gradient solver, have to be used.

Still accuracy **criteria** with respect to the choice of Δs and Δt have to be observed by the modeler in order to avoid excessive numerical diffusion (also called numerical dispersion) and numerical oscillations.

In order to **reduce numerical diffusion**, which means that the discretization is able to adequately represent sharp thermal fronts without smearing, it is required that the advective heat flux is smaller than the dispersive and diffusive heat fluxes everywhere within the solution domain. For extreme cases, this requirement can be stated heuristically as

$$C_w q \frac{T}{2} \leq (\lambda_m + C_w D_{t,disp,L}) \frac{T}{\Delta s} \tag{4.27}$$

This leads to the **requirement for the spatial discretization** Δs:

$$\Delta s \leq \frac{2 \cdot \left(\frac{\lambda_m}{C_w} + D_{\mathrm{t,disp,L}} \right)}{q} = \frac{2D_t}{q} \tag{4.28}$$

For **dominant macrodispersion**, the criterion reduces to

$$\Delta s \leq 2\beta_{\mathrm{L}} \tag{4.29}$$

An equivalent formulation is that the **thermal grid Peclet number** satisfies the following:

$$\mathrm{Pe} = \frac{q\Delta s}{D_{\mathrm{t}}} \leq 2 \tag{4.30}$$

In order to **reduce numerical oscillations** of the solution, which manifest themselves as overshooting and undershooting, it is required that the advective heat flux into any cell is smaller than the rate of change of energy within the cell. For extreme cases, this requirement can be stated heuristically as

$$C_{\mathrm{w}} q T \leq \frac{C_{\mathrm{m}} T \Delta s}{\Delta t} \tag{4.31}$$

This leads to the **requirement for the time step**:

$$\Delta t \leq \frac{C_{\mathrm{m}} \Delta s}{C_{\mathrm{w}} q} \tag{4.32}$$

An equivalent formulation is that the **thermal grid Courant number** Co satisfies the **Courant–Friedrichs–Lewy stability condition**:

$$\mathrm{Co} = \frac{C_{\mathrm{w}} q \Delta t}{C_{\mathrm{m}} \Delta s} \leq 1 \tag{4.33}$$

Compared to solute transport, the criterion is relaxed by the thermal retardation factor.

Still **lateral numerical diffusion** has to be controlled. From experience with solute plume simulations, it is desirable to resolve the thermal plume laterally by at least 10 cells.

Finally, it is recommended to check whether the numerical results are **grid convergent**. This means that the results using a finer grid are practically invariant compared to the original grid. An **application** of the finite difference method is given, for example, in Birkholzer and Tsang (2000).

4.2.2 Principles of the finite element method for heat transport

In the finite element method, discretization uses the so-called **finite elements** (e.g., prismatic elements; Figure 4.7). Various classes of finite elements are available. Each element contains a number of **nodal points**, where the approximate solution is sought. The simplest two-dimensional and three-dimensional finite elements are triangular (3 nodal points) and tetrahedral (4 nodal points) elements with linear interpolation functions. Due to their flexible shape, finite element grids can much better adapt to irregular boundaries of the domain D and can also be better refined locally in regions where better resolution is needed, for example, close to sources and sinks. Within the solution domain, a **trial solution** is defined as follows:

$$\hat{T}(\mathbf{x},t) = \sum_{i=1}^{n} T_i(t) w_i(\mathbf{x}) \tag{4.34}$$

The functions $w_i(\mathbf{x})$ are **weighting functions**, which are determined from **the interpolation functions** of the finite element, and n is the number of nodal points. In fact, $w_i(\mathbf{x})$ vanishes outside the neighborhood of a nodal point (element patch containing all elements connected to the nodal point).

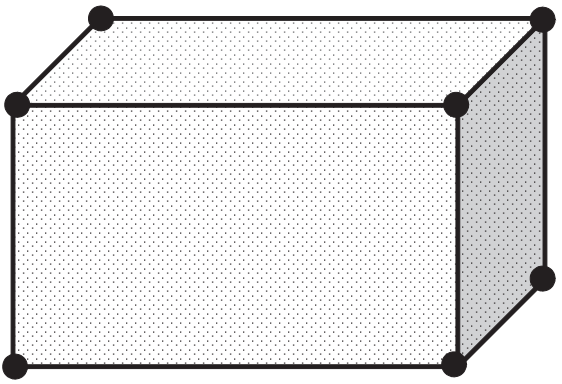

Figure 4.7 Prismatic finite element with nodal points.

The parameters $T_i(t)$ are the **unknown nodal values**. The trial solution approximates the temperature distribution within the domain. Inserting the trial solution into the rearranged heat transport equation:

$$L(\hat{T}) = \nabla \cdot \left[\mathbf{D}_t \nabla \hat{T} \right] - \frac{C_w}{C_m} \nabla \cdot \left(\mathbf{q} \hat{T} \right) + \frac{P_t}{C_m} - \frac{\partial \hat{T}}{\partial t} = \varepsilon(\mathbf{x}, t) \tag{4.35}$$

yields a **residual** $\varepsilon(\mathbf{x}, t)$. According to **Galerkin**, it is required that the **weighted residual** using $w_i(\mathbf{x})$ as a weighting function **vanishes in the neighborhood of all nodal points** i with unknown variable T:

$$\int_D \varepsilon(\mathbf{x}, t) w_i(\mathbf{x}) \, \mathrm{d}D = 0; \quad i = 1, ...n \tag{4.36}$$

Integration is, in fact, restricted to the element patch of each nodal point. Therefore, the condition states that the weighted residual vanishes in the neighborhood of each nodal point. To avoid the appearance of distributions, one integration step of the conduction-thermal dispersion term is carried over to the weighting function using Greene's theorem. Integration (analytical if possible or numerical using Gauss points) yields a **set of ordinary differential equations** as follows:

$$\sum_{j=1}^{n} F_{ij}(t^*) \left(\frac{\mathrm{d}T_j}{\mathrm{d}t} \right) + \sum_{j=1}^{n} A_{ij}(t^*) T_j = b_i; \quad i = 1, ..., n \tag{4.37}$$

where A_{ij} and F_{ij} are matrix elements and b_i is a constant term. Still it has to be decided for which time t^* the matrices are evaluated. For a fully **implicit scheme** $t^* = t + \Delta t$, and for a **Crank–Nicolson scheme** $T(t^*) = 0.5 \cdot (T(t + \Delta t) + T(t))$. Since the matrix [F] is not a diagonal matrix, an explicit scheme does not provide a computational advantage, unless [F] is diagonalized by lumping all terms of a row in the diagonal. The **time derivative** is often discretized in finite differences with:

$$\frac{\mathrm{d}T_j}{\mathrm{d}t} \simeq \frac{T_j(t + \Delta t) - T_j(t)}{\Delta t} \tag{4.38}$$

leading to a linear equation system for the unknown nodal values $T_j(t + \Delta t)$ of the temperature. The resulting **matrix** [A] is again sparse, since only the neighboring nodal points are involved in the integration. Again, in general, the matrix [A] is **not symmetric** due to the advective terms. Adapted numerical techniques, like the biconjugate gradient solver, have to be used.

An alternative consists of using an explicit scheme for the advective term and an implicit scheme for the diffusive–dispersive term, which leads to a symmetric matrix [A] (e.g., Leismann and Frind 1989).

Finite element techniques exhibit similar **numerical stability problems** as the finite difference methods. Again, the **grid Peclet number** (Equation 4.30) and the **Courant number** (Equation 4.33) **criteria** have to be observed. In order to avoid lateral numerical diffusion, finite element grids can be aligned along water flow lines leading to the principal direction technique (Frind and Germain 1986). This avoids lateral numerical diffusion. An **application** of the finite element method is given, for example, in Molson et al. (1992).

4.2.3 Principles of the finite volume method for heat transport

In the finite volume method, the solution domain is divided into small (convex) **finite volumes**. Nodal points are used to interpolate the field variable. Usually a single node is used for each finite volume. **Surface heat fluxes** are expressed either by Gauss' divergence theorem or directly by approximating the fluxes. The sum of all inflowing heat fluxes is equal to the rate of change of energy within the finite volume according to heat conservation. Boundary fluxes (Neumann type boundary conditions) can be directly introduced into the balance equation. **For grids using rectangular blocks as finite volumes, the approach is identical to the finite difference approach** as described in Section 4.2.1. However, the finite volume method is **more general** and allows unstructured grids. A model formulation using the finite volume method can be found in Russell et al. (2003). **Applications** of the finite volume method are given in Clauser (2003) and Rühaak et al. (2008).

4.2.4 Principles of the method of characteristics for heat transport

In the **method of characteristics** used for transport problems in groundwater, the transport step is split into two half steps (operator splitting), one purely advective and the other diffusive and dispersive. In a **moving control volume**, moving with the thermal front velocity $\mathbf{u}_t$, the change of temperature can be expressed as follows:

$$\begin{aligned}\frac{\mathrm{d}T}{\mathrm{d}t} &= \frac{\partial T}{\partial t} + \frac{\partial T}{\partial x}\frac{\partial x}{\partial t} + \frac{\partial T}{\partial y}\frac{\partial y}{\partial t} + \frac{\partial T}{\partial z}\frac{\partial z}{\partial t} \\ &= \frac{\partial T}{\partial t} + \frac{\partial T}{\partial x}u_{\mathrm{t},x} + \frac{\partial T}{\partial y}u_{\mathrm{t},y} + \frac{\partial T}{\partial z}u_{\mathrm{t},z}\end{aligned} \tag{4.39}$$

The resulting tracks $x(t)$, $y(t)$, and $z(t)$ of the particles are called the **characteristics**. The **diffusive and dispersive half time step** is treated with the **conventional finite difference method**, whereas the **advection half time step** is performed using **particle tracking** based on the velocity field. A large number of particles are initially introduced in the solution domain. Each particle carries a temperature, which can change over time. The **principal steps** are as follows:

- Given temperature $T_p(t)$ of particles and $T_{ij}(t)$ of cells.
- All particles are moved advectively. New intermediate cell temperatures $T_{ij}^*(t+\Delta t)$ are calculated by averaging the particle temperatures in the cells.
- Purely diffusive and dispersive temperature changes are calculated on the finite difference grid using $T_{ij}^*(t+\Delta t)$, yielding new cell temperatures $T_{ij}(t + \Delta t)$.
- New particle temperature values $T_p(t + \Delta t)$ are calculated by adding increments.
- Start a new time step.

It is important that an optimal **interpolation of the velocity** within the cells is obtained. Frequently used interpolation schemes follow Prickett et al. (1981) and Pollock (1988). Modified (e.g., Liu and Dane 1996) and hybrid (forward and backward) schemes of the method of characteristics do exist. Numerical oscillations of the solution occur due to the particle-based nature of the method. Increasing the number of particles in the system can reduce these oscillations.

An **application** is presented, for example, in Hecht-Méndez et al. (2010).

4.2.5 Principles of the random walk method for heat transport

In the **random walk method** used for transport problems in groundwater, the transport step is again split into two half steps, one purely advective and the other diffusive and dispersive as in the method of characteristics. Again, the **advective time step** is performed by **particle tracking,** based on the velocity field. In contrast to the method of characteristics, the particles carry a fixed energy in the random walk method. A large ensemble of particle paths yields, in the limit, the solution of the transport equation. From the analytical solution of the transport problem for uniform flow velocity in the direction of x, the **new particle position** after a time step Δt, starting at the location $x(t = 0) = x_0$, is

$$x_p(t+\Delta t) = x_p(t) + u_{t,x}\,\Delta t + Z\sqrt{2\,D_{t,L}\,\Delta t} \tag{4.40}$$

where Z is a normally distributed random number with zero average and standard deviation $\sigma_Z = 1$. The y- and z-components are obtained in a similar manner using transversal coefficients. The method yields a distribution

of particles of equal energy. The cell temperature is obtained by counting the particles within a cell and dividing the total energy by the total heat capacity of the aquifer volume in the cell. Therefore, enough particles have to be added to the system. Since Equation 4.40 is based on a uniform velocity field, which is not the general case, **correction terms** have to be added (referred to as Fokker–Planck terms). The **new particle position** is for two-dimensional heat transport:

$$x_{\mathrm{p}}(t+\Delta t) = x_{\mathrm{p}}(t) + \left[u_{t,x} + \frac{\partial D_{\mathrm{t},xx}}{\partial x} + \frac{\partial D_{\mathrm{t},xy}}{\partial y} \right]_{(\mathbf{x}_{\mathrm{p}}(t))} \cdot \Delta t + Z' \cdot \left[\sqrt{2D_{\mathrm{t,L}}\Delta t}\, \frac{u_{\mathrm{t},x}}{u_{\mathrm{t}}} \right]_{(\mathbf{x}_{\mathrm{p}}(t))} - Z'' \cdot \left[\sqrt{2D_{\mathrm{t,T}}\Delta t}\, \frac{u_{\mathrm{t},y}}{u_{\mathrm{t}}} \right]_{(\mathbf{x}_{\mathrm{p}}(t))}$$

$$y_{\mathrm{p}}(t+\Delta t) = y_{\mathrm{p}}(t) + \left[u_{\mathrm{t},y} + \frac{\partial D_{\mathrm{t},yx}}{\partial x} + \frac{\partial D_{\mathrm{t},yy}}{\partial y} \right]_{(\mathbf{x}_{\mathrm{p}}(t))} \cdot \Delta t + Z' \cdot \left[\sqrt{2D_{t,L}\Delta t}\, \frac{u_{t,y}}{u_{t}} \right]_{(\mathbf{x}_{\mathrm{p}}(t))} + Z'' \cdot \left[\sqrt{2D_{\mathrm{t,T}}\Delta t}\, \frac{u_{\mathrm{t},x}}{u_{\mathrm{t}}} \right]_{(\mathbf{x}_{\mathrm{p}}(t))} \tag{4.41}$$

where u_{t} is the absolute value of the thermal velocity, and Z' as well as Z'' are normally distributed random numbers (zero mean and unit standard deviation). The correction term prevents, for example, particles from accumulating at stagnation points (Kinzelbach 1987). It is again important that an optimal **interpolation of the velocity** within the cells is obtained. Frequently used interpolation schemes are after Prickett et al. (1981) and after Pollock (1988). For continuous injection of heat, particles have to be added continuously. A three-dimensional formulation for solute transport by random walk can be found in Kinzelbach and Uffink (1991) and Lichtner et al. (2002). A two-dimensional **application** in heat transport is presented in Chevalier and Banton (1999).

4.3 STRATEGY FOR COUPLED FLOW AND HEAT TRANSPORT

Usually, **coupled flow and heat transport equations** are linearized using a **Picard iteration scheme** (point iteration). In a first step, the flow equation is solved. Based on the head values, the Darcy velocity field is evaluated in a second step. In a third step, the heat transport equation is solved, and in a fourth step, the temperature-dependent parameters like water density are updated. All four steps are iterated to a specified convergence tolerance.

Various codes are organized in this manner (see Ackerer et al. 2004; Molson and Frind 2012). Molson et al. (1992) handle nonlinearities in the coupled flow and heat transport equations by centering the nonlinear terms in time during the iteration. In order to speed up the iteration process, Ackerer et al. (2004) suggest that the heat transport equation is evaluated first, and then an update of the temperature-dependent parameters is performed followed by solving the flow equation with the evaluation of the velocity field. In their scheme, the heat transport equation is solved with velocities defined in the previous iteration. Because the flow equation is more dependent on the temperature than the heat transport equation on the heads (temperature variations in time create a sink/source term in the flow equation), this algorithm should reduce the number of iterations needed within one time step. However, the **solution of highly nonlinear, density-dependent flow problems** involving high temperature contrasts may require other solution approaches (see, e.g., Herbert et al. 1988).

Diersch and Kolditz (1998) use **first- or second-order predictor–corrector schemes** for solving the coupled equations.

4.4 SOME AVAILABLE CODES FOR THERMAL TRANSPORT MODELING IN GROUNDWATER

As already stated, a **large number of codes on solute and contaminant transport** are available, such as MT3D (Zheng 1990) or MT3DMS (Zheng and Wang 1999), which, in principle, can also be used for thermal transport studies in groundwater by analogy. Among the codes that directly allow simulation of thermal processes, we mention a few. A list of some selected groundwater flow and heat transport codes are presented in Anderson (2005).

FEFLOW (DHI-WASY 2010) is a variably saturated, three-dimensional finite element code for the simulation of variable-density water flow, solute, and heat transport, including coupled transport. Thermal applications are presented, for example, in Maréchal et al. (1999) and Nam et al. (2008). The software includes analytical and numerical modules for the finite element formulation of BHEs in modeling geothermal heating systems.

HST3D (Kipp 1997) is a three-dimensional finite difference code. It simulates groundwater flow and associated heat and solute transport in saturated aquifers. It can handle variable water density and viscosity. Among other applications, the code is offered for heat storage in aquifers. An application using the code is given in Bravo et al. (2002).

HEATFLOW-SMOKER (Molson and Frind 2012) is a three-dimensional finite element code for solving complex density-dependent groundwater flow and thermal energy transport problems. The model can be used to solve one-, two-, or three-dimensional heat transport problems within a variety of hydrogeological systems, including discretely fractured porous media.

HydroGeoSphere (Graf and Therrien 2007; Raymond et al. 2011) is a three-dimensional numerical model for fully integrated density-dependent subsurface and surface flow, heat transport, and solute transport. It was used by Raymond et al. (2011) for a numerical analysis of thermal response tests. A review was presented by Brunner and Simmons (2012).

SEAWAT (Langevin et al. 2007) is a coupled version of MODFLOW and MT3DMS models designed to simulate three-dimensional, variable-density, groundwater flow and solute transport in saturated porous media. The effects of fluid viscosity variation on groundwater flow are included. Although not explicitly designed to model heat transport, temperature can be simulated as one of the species by entering appropriate transport coefficients. Version 4 is based on MODFLOW-2000 and MT3DMS. Applications are presented, for example, in Vandenbohede and Lebbe (2011).

SHEMAT (Clauser 2003) is a three-dimensional finite difference code. It mainly focuses on numerical simulation of reactive flow in geothermal aquifers. It solves transient coupled problems of groundwater flow, heat transport, species transport, and chemical water–rock interaction in fluid-saturated porous media. Applications are presented, for example, in Clauser (2003) and Pannike et al. (2006).

SPRING (delta-h 2012) is a variably saturated three-dimensional finite element code for the simulation of coupled water flow and solute or heat transport in saturated and unsaturated porous media. An application is shown, for example, in Engeler et al. (2011).

SUTRA (Voss and Provost 2010) is a variably saturated three-dimensional finite element code for density-dependent saturated or unsaturated groundwater flow, and solute or heat transport. An application is presented, for example, in Ronan et al. (1998).

TOUGH2 (Pruess et al. 2012) is a variably saturated three-dimensional integral finite difference code for nonisothermal flows of multicomponent, multiphase fluids and coupled heat transfer in one-, two-, and three-dimensional porous and fractured media. Temperature and pressure dependence of thermophysical properties are taken into account. Main applications for which TOUGH2 was designed are in geothermal reservoir engineering, nuclear waste disposal, environmental assessment and remediation, and unsaturated and saturated zone hydrology. A thermal application is presented, for example, in Birkholzer and Zhang (2000).

VS2DI (Hsieh et al. 2000) is a two-dimensional finite difference code for simulating fluid flow and solute or heat transport in variably saturated porous media in one or two dimensions using Cartesian or radial coordinate systems. An application is given, for example, in Constantz (1998).

Table 4.1 gives an **overview on various codes** that are suited for heat transport simulations of shallow geothermal systems considering groundwater flow.

Table 4.1 Numerical codes suitable for heat transport simulations of shallow geothermal systems considering groundwater flow (not meant to be exhaustive or complete)

Code name	*Numerical method*	*Processes*	*Coupling*	*Availability*	*Comments*	*Reference*
AST/TWOW	FD	H,T	H → T	Commercial	3D, calculates near-field heat transport around BHEs	Schmidt and Hellström (2005)
BASIN2	FD	H,T	H ↔ T, M, CH	Free code	2D, simulates sedimentary basin development; cross-sectional view	Bethke et al. (2007)
COMSOL	FE	H, T, C	H ↔ T	Commercial	3D, multiphysics (more processes can be coupled)	Holzbecher and Kohfahl (2008)
FEFLOW	FE	H, T, C	H ↔ T, M, C	Commercial	2D, 3D	DHI-WASY (2010)
FRACHEM	FE	H, T, C	H ↔ T, M, C	Scientific	3D, used for hot dry rock modeling	Bächler (2003)
FRACture	FE	H,T	H ↔ T, M	Scientific	3D, developed for hot dry rock modeling	Kohl and Hopkirk (1995)
ROCKFLOW/GeoSys	FE	H, T, C	H ↔ T, C	Scientific	3D, fracture systems can be included. Allows for multiphase flow	Kolditz et al. (2001)
HEATFLOW-SMOKER	FE	H,T	H ↔ T	Free code	1D, 2D, 3D	Molson and Frind (2012)
HST2D/3D	FD	H, T, C	H ↔ T, M, R	Free code	2D, 3D	Kipp (1997)

HydroTherm	FE	H,T	H ↔ T	Free code	2D, 3D, two-phase model; can simulate 0 to 1200°C	Kipp et al. (2008)
HydroGeoSphere	FV	H,T, C	H ↔ T, C	Scientific	3D	Raymond et al. (2011)
HYDRUS-2D/3D	FE	H,T, C	H → T	Commercial	Unsaturated zone, plant water uptake is considered	Radcliffe and Šimůnek (2010)
SEAWAT	FD	H,T, C	H ↔ T, C	Free code	3D	Langevin et al. (2008)
SHEMAT	FD	H,T, C	H ↔ T, C	Commercial	3D	Clauser (2003)
SUTRA	FE	H,T, C	H ↔ T, C	Free code	2D, 3D	Voss and Provost (2010)
SPRING	FE	H,T, C	H ↔ T, C	Commercial	3D	delta-h (2012)
THETA	FD	H,T, C	H ↔ T, C	Scientific	3D	Kangas (1996)
TOUGH2	FD	H,T, C	H ↔ T, M, R	Commercial	1D, 2D, and 3D, one of the most widely used codes in geothermal energy technologies; allows for multiphase flow	Pruess et al. (2012)
TRADIKON 3D	FD	H,T	H → T	Free code	3D, specially designed for BHE assessments	Brehm (1989)
VS2DI	FD	H,T	H → T	Free code	2D	Hsieh et al. (2000)

Source: After Hecht-Méndez, J. et al. *Ground Water* 48(5), 741–756, 2010.

Notes: C, contaminant (solute); H, hydraulic; H → T, fluid flow is independent of T; H ↔ T, fluid flow depends on T; T, temperature; M, mechanical deformation (pore deformation); R, chemical reaction.

REFERENCES

Ackerer, P., Younès, A., Mancip, M. (2004). A new coupling algorithm for density driven flow in porous media. *Geophysical Research Letters* 31, L12506, doi:10.1029/2004GL019496.

Al-Khoury, R. (2012). *Computational Modeling of Shallow Geothermal Systems*. CRC-Press/Baalkema, Taylor and Francis Group, Boca Raton, USA.

Al-Khoury, R., Bonnier, P.G., Brinkgreve, R.B.J. (2005). Efficient finite element formulation for geothermal heating systems. Part I: Steady-state. *International Journal for Numerical Methods in Engineering* 63, 988–1013.

Al-Khoury, R., Bonnier, P.G. (2006). Efficient finite element formulation for geothermal heating systems. Part II: Transient. *International Journal for Numerical Methods in Engineering* 67, 725–745.

Al-Khoury, R., Köbel, T., Schramedei, R. (2010). Efficient numerical modeling of heat exchangers. *Computers and Geosciences* 36, 1301–1315.

Anderson, M.P. (2005). Heat as a groundwater tracer. *Ground Water* 43(6), 951–968.

Bächler, D. (2003). Coupled thermal-hydraulic-chemical modeling at the Soultz-sous-Forêts HDR Reservoir (France). Ph.D. diss., Swiss Federal Institute of Technology, Zurich.

Bauer, D., Heidemann, W., Müller-Steinhagen, H., Diersch, H.-J.G. (2011). Thermal resistance and capacity models for borehole heat exchangers. *International Journal of Energy Research* 35, 312–320.

Bethke, C., Lee, M.-K., Park, J. (2007). *Basin Modeling with Basin2, Release 5.0.1*. Hydrogeology Program, University of Illinois, Urbana Champaign, Illinois.

Birkholzer, J.T., Zhang, Y.W. (2000). Modeling the thermal-hydrologic processes in a large-scale underground heater test in partially saturated fractured tuff. *Water Resources Research* 36(6), 1431–1447.

Bravo, H.R., Feng, J., Hunt, R.J. (2002). Using groundwater temperature data to constrain parameter estimation in a groundwater flow model of a wetland system. *Water Resources Research* 38(8), 28-1–28-14, doi:10.1029/2000WR000172.

Brehm, D. (1989). *Development, Validation and Application of a 3-Dimensional, Coupled Flow and Transport Finite Differences Model*. Giessener Geologische Schriften, Giessen, Lenz Verlag.

Brookfield, A.E., Sudicky, E.A., Parks, Y.-J., Conant, B. (2009). Thermal transport modelling in a fully integrated surface/subsurface framework. *Hydrological Process* 23(15), 2150–2164.

Brunner, P., Simmons, C.T. (2012). HydroGeoSphere: A fully integrated, physically based hydrological model. *Ground Water* 50(2), 170–176.

Chevalier, S., Banton, O. (1999). Modelling of heat transfer with the random walk method. Part 1. Application to thermal energy storage in porous aquifers. *Journal of Hydrology* 222, 129–139.

Chiang, W.-X., Kinzelbach, W. (2005). *2D Groundwater Modeling with PMWIN: A Simulation System for Modeling Flow and Transport Processes*. Springer, Berlin, 2005.

Chiasson, A.D., Rees, S.J., Spitler, J.D. (2000). A preliminary assessment of the effects of groundwater flow on closed-loop ground source heat pump systems. *ASHRAE Transactions* 106(1), 380–393.

Clauser, C. (Ed.) (2003). *Numerical Simulation of Reactive Flow in Hot Aquifers—SHEMAT and Processing SHEMAT*. Springer, Berlin.

Constantz, J. (1998). Interaction between stream temperature, streamflow, and groundwater exchanges in alpine streams. *Water Resources Research* 34(7), 1609–1616.

Delta-h (2012). *SPRING 4 Online Manual*. Delta-h, Witten, Germany.

Deng, Z., Rees, S.J., Spitler, J.D. (2005). A model for annual simulation of standing column well ground heat exchangers. *HVAC&R Research* 11, 637–656.

DHI-WASY (2010). *FEFLOW 6. User Manual*. DHI-WASY GmbH, Berlin, Germany.

Diersch, H.-J.G. (1996). Interactive, graphics-based finite-element simulation system FEFLOW for modeling groundwater flow, contaminant mass and heat transport processes. User's Manual Version 4.5, April 1996, WASY Institute for Water Resources Planning and Systems Research Ltd, Berlin. DHI-WASY GmbH, DHI-WASY GmbH, Berlin, Germany.

Diersch, H.-J., Kolditz, O. (1998). Coupled groundwater flow and transport: 2. Thermohaline and 3D convection systems. *Advances in Water Resources* 21, 401–425.

Diersch, H.-J.G., Bauer, D., Heidemann, W., Rühaak, W., Schätzl, P. (2011a). Finite element modeling of borehole heat exchanger systems. Part I Fundamentals. *Computers and Geosciences* 37, 1122–1135.

Diersch, H.-J.G., Bauer, D., Heidemann, W., Rühaak, W., Schätzl, P. (2011b). Finite element modeling of borehole heat exchanger systems. Part II. Numerical simulations. *Computers and Geosciences* 37, 1136–1147.

Doughty, C., Hellström, G., Tsang, C.F., Claesson, J. (1982). A dimensionless parameter approach to the thermal behaviour of an aquifer thermal energy storage system. *Water Resources Research* 18(3), 571–587.

Dwyer, T.E., Eckstein, Y. (1987). Finite-element simulation of low-temperature, heat-pump-coupled, aquifer thermal energy storage. *Journal of Hydrology* 95, 19–38.

Engeler, I., Hendricks Franssen, H.J., Müller, R., Stauffer, F. (2011). The importance of coupled modelling of variably saturated groundwater flow-heat transport for assessing river-aquifer interactions. *Journal of Hydrology* 397, 295–305.

Fan, R., Jiang, J., Yao., Y., Shiming, D., Ma, Z. (2007). A study of the performance of a geothermal heat exchanger under coupled heat conduction and groundwater advection. *Energy* 32, 2199–2209.

Ferguson, G. (2007). Heterogeneity and thermal modeling in ground water. *Ground Water* 45(4), 485–490.

Frind, E.O., Germain, D. (1986). Simulation of contaminant plumes with large dispersive contrast: Evaluation of alternating direction Galerkin models. *Water Resources Research* 22(13), 1857–1873.

Fujimitsu, Y., Fukuoka, K., Ehara, S., Takeshita, H., Abe, F. (2010). Evaluation of subsurface thermal environment change caused by a ground-coupled heat pump system. *Current Applied Physics* 11 (1) Supplement S113–S116.

Gao, Q., Zhou, X.-Z., Jiang, J., Chen, X.-L., Yan, Y.-Y. (2013). Numerical simulation of the thermal interaction between pumping and injecting well groups. *Applied Thermal Engineering* 51, 10–19.

Glück, B. (2011). Simulationsmodell Erdwärmesonden zur wärmetechnischen Beurteilung von Wärmequellen, Wärmesenken und Wärme/Kältespeichern (in German) (Simulation model for BHE for the assessment of heat sources and sinks and heat storage). www.berndglueck.de.

Graf, T., Therrien, R. (2007). Coupled thermohaline groundwater flow and single-species reactive solute transport in fractured porous media. *Advances in Water Resources* 30, 742–771.

Hecht-Méndez, J., Molina-Giraldo, N., Blum, P., Bayer, P. (2010). Evaluating MT3DMS for heat transport simulation of closed geothermal systems. *Ground Water* 48(5), 741–756.

Herbert, A.W., Jackson, C.P., Lever, D.A. (1988). Coupled groundwater flow and solute transport with fluid density strongly dependent upon concentration. *Water Resources Research* 24(10), 1781–1795.

Hidalgo, J.J., Carrera, J., Dentz, M. (2009). Steady state heat transport in 3D heterogeneous porous media. *Advances in Water Resources* 32(8), 1206–1212.

Holzbecher, E., Kohfahl, C. (2008). *Geothermics Modelling using COMSOL Multiphysics*. Seminar manual. Berlin.

Hsieh, P.A., Wingle, W., Healy, R.W. (2000). VS2DI-A graphical software package for simulating fluid flow and solute or energy transport in variably saturated porous media. USGS Water Resources Investigations Report 9, 9-4130. USGS, Denver, Colorado.

Jalaluddin, Miyara, A. (2012). Thermal performance investigation of several types of vertical ground heat exchangers with different operation mode. Applied Thermal Engineering 33–34, p. 167–174. doi: 10.1016/j.applthermaleng.2011.09.030.

Kangas, M.T. (1996). Modeling of transport processes in porous media for energy applications. Ph.D. thesis, Helsinki University of Technology, Helsinki, Finland.

Kim, J., Lee, Y., Yoon, W.S., Yeon, Y.S., Koo, M.-H., Keehm, Y. (2010). Numerical modeling of aquifer thermal energy storage systems. *Energy* 35, 4955–4965.

Kinzelbach, W. (1987). *Numerische Methoden zur Modellierung des Transports von Schadstoffen im Grundwasser. Schriftenreihe GWF Wasser-Abwasser*. Vol. 21, Oldenburg Verlag, Munich, Germany.

Kinzelbach, W., Uffink, G. (1991). The random walk method and extensions in groundwater modelling. In: Transport Processes in Porous Media, J. Bear and M.Y. Corapcioglu (eds.), Kluwer Academic Publishers, Dordrecht, The Netherlands, pp. 761–787.

Kipp, K.L. (1997). Guide to the revised heat and solute transport simulator: HST3D—Version 2. Water-Resources Investigations Report 97-4157, USGS, Denver, Colorado.

Kipp, K.L., Jr., Hsieh, P.A., Charlton, S.R. (2008). Guide to the revised groundwater flow and heat transport simulator: HYDROTHERM—Version 3: U.S. Geological Survey Techniques and Methods 6-A25, 160 p.

Kohl, T., Hopkirk, R.J. (1995). FRACTure—A simulation code for forced fluid flow and transport in fractured rock. *Geothermics* 24(3), 333–343.

Laloui, L., Nuth, M., Vulliet, L. (2006). Experimental and numerical investigations of the behavior of a heat exchanger pile. *International Journal for Numerical and Analytical Method in Geomechanics* 30, 763–781.

Langevin, C.D., Thorne, D.T., Jr., Dausman, A.M., Sukop, M.C. Guo, W. (2008). SEAWAT Version 4: A Computer program for simulation of multi-species solute and heat transport. *U.S. Geological Survey Techniques and Methods*. Book 6, Chap. A22. USGS, Reston, Virginia.

Lazzari, S., Priarone, A., Zanchini, E. (2010). Long-term performance of BHE (borehole heat exchanger) with negligible groundwater flow. *Energy* 35, 4966–4974.

Lee, C.K., Lam, H.N. (2008). Computer simulation of borehole ground heat exchangers for geothermal heat pump systems. *Renewable Energy* 33, 1286–1296.

Leismann, H.M., Frind, E.O. (1989). A symmetric-matrix time integration scheme for the efficient solution of advection-dispersion problems. *Water Resources Research* 25(6), 1133–1139.

Lichtner, P.C., Kelkar, S., Robinson, B. (2002). New form of dispersion tensor for axisymmetric porous media with implementation in particle tracking. *Water Resources Research* 38(8), 1146, doi:10.1029/2000WR000100.

Lippmann, M.J., Tsang, C.F., Witherspoon, P.A. (1977). Analysis of the response of geothermal reservoirs under injection and production procedures. SPE Paper No. 6537.

Liu, H.H., Dane, J.H. (1996). An interpolation-corrected modified method of characteristics to solve advection-dispersion equations. *Advances in Water Resources* 19(6), 359–368.

Maréchal, J.C., Perrochet, P., Tacher, L. (1999). Longterm simulations of thermal and hydraulic characteristics in a mountain massif: The Mont Blanc case study, French and Italian Alps. *Hydrogeology Journal* 7(4), 341–354.

Mercer, J.W., Faust, C.R., Miller, W.J., Pearson, F.J., Jr. (1982). Review of simulation techniques for aquifers thermal energy storage (ATES). *Advances in Hydroscience* 13, 1–129. Academic Press, New York.

Mercer, J.W., Pinder, G.F., Donaldson, I.G. (1975). A Galerkin finite element analysis of the hydrothermal system at Wairakei, New Zealand. *Journal of Geophysical Research* 80(17), 2608–2621.

Merheb, F. (1984). Modèle de gestion des echanges hydrothermiques dans les nappes souterraines: Application à la région de Strasbourg. PhD Thesis Université Lous Pasteur de Strasbourg, Institut de Mécanique des Fluides.

Molson, J.W., Frind, E.O. (2012). HEATFLOW-SMOKER, Density-dependent flow and advective -dispersive transport of thermal energy, mass or residence time in three-dimensional porous or fractured porous media. User guide. Version 5.0, University of Laval and University of Waterloo, Canada.

Molson, J.W., Frind, E.O., Palmer, C.D. (1992). Thermal energy storage in an unconfined aquifer 2. Model development, validation, and application. *Water Resources Research* 28(19), 2857–2867.

Nam, Y., Ooka, R., Whang, S. (2008). Development of a numerical model to predict heat exchange rates for a ground-source heat pump system. *Energy and Buildings* 40, 2133–2140.

Painter, S., Seth, M.S. (2003). MULTIFLO User's Manual; MULTIFLO Version 2.0. Southwest Research Institute, San Antonio, Texas.

Pannike, S., Kölling, M., Panteleit, P., Reichling, J., Scheps, V., Schulz, H.D. (2006). Auswirkung hydrogeologischer Kenngrössen auf die Kältefahnen von Erdwärmesondenanlagen in Lockersedimenten. *Grundwasser* 11(1), 6–18.

Park, H., Lee, S.-R., Yoon, S., Choi, J.-C. (2013). Evaluation of thermal response and performance of PHC energy pile: Field experiments and numerical simulations. *Applied Energy* 103, 12–24.

Park, H., Lee, S.-R., Yoon, S., Shin, H., Lee, D.-S. (2012). Case study of heat transfer behavior of helical ground heat exchanger. *Energy and Buildings* 53, 137–144.

Parlange, M.B., Cahill, A.T., Nielsen, D.R., Hopmans, J.W., Wendroth, O. (1998). Review of heat and water movement in field soils. *Soil & Tillage Research* 47, 5–10.

Philip, J.R., de Vries, D.A. (1957). Moisture movement in porous materials under temperature gradients. *Transactions American Geophysical Union* 38, 222–232.
Pollock, D.W. (1988). Semianalytical computation of path lines of finite difference models. *Ground Water* 26(6), 743–750.
Prickett, T.A., Naymik, T.G., Lonnquist, C.G. (1981). A "random walk" transport model for selected groundwater quality evaluations. *Illinois State Water Survey Bulletin* 65.
Pruess, K., Oldenburg, C., Moridis, G. (2012). TOUGH2 User's Guide, Version 2.1. Report LBNL-43134 (revised), Lawrence Berkeley National Laboratory, Berkeley, California.
Radcliffe, D., Simůnek, J. (2010). *Soil Physics with HYDRUS. Modeling and Applications*. CRC Press, Boca Raton, Florida.
Raymond, J., Therrien, R., Gosselin, L., Lefebvre, R. (2011). Numerical analysis of thermal response tests with a groundwater flow and heat transfer model. *Renewable Energy* 36, 315–324.
Ronan, A.D., Prudic, D.E., Thodal, C.E., Constantz, J. (1998). Field study and simulation of diurnal temperature effects on infiltration and variably saturated flow beneath an ephemeral stream. *Water Resources Research* 34(9), 2137–2153.
Rühaak, W., Rath, V., Wolf, A., Clauser, C. (2008). 3D finite volume groundwater and heat transport modeling with non-orthogonal grids, using a coordinate transformation method. *Advances in Water Resources* 31(3), 513–524.
Russell, T.F., Heberton, C.I., Konikow, L.F., Hornberger, G.Z. (2003). A finite-volume ELLAM for three-dimensional solute-transport modelling. *Ground Water* 41(2), 258–272.
Sauty, J.P., Gringarten, A.C., Menjoz, A., Landel, P.A. (1982). Sensible energy storage in aquifers. 1. Theoretical study. *Water Resources Research* 18(2), 245–252.
Schmidt, T., Hellström, G. (2005). Ground source cooling—Working paper on usable tools and methods. EU Commission SAVE Programme and Nordic Energy Research.
Seo, H.S., Šimůnek, J., Poeter, E.P. (2007). Documentation of the HYDRUS package for MODFLOW-2000, the U.S. Geological Survey modular ground-water model, GWMI 2007-01. Int. Ground Water Modeling Ctr., Colorado School of Mines, Golden.
Sidiropoulos, E., Tzimopoulos, C. (1983). Sensitivity analysis of a coupled heat and mass transfer model in unsaturated porous media. *Journal of Hydrology* 64, 281–298.
Signorelli, S., Bassetti, S., Pahud, D., Kohl, T. (2007). Numerical evaluation of thermal response tests. *Geothermics* 36, 141–166.
Sophocleous, M. (1979). Analysis of water and heat flow in unsaturated-saturated porous media. *Water Resources Research* 15(5), 1195–1206.
Sun, Z.F., Carrington, C.G. (1995). A new numerical scheme for convective dominated heat transfer in a porous medium with strong temperature gradients. *Transport in Porous Media* 21, 101–122.
Tsang, C.F., Buschek, T., Doughty, C. (1981). Aquifer thermal energy storage: A numerical simulation of Auburn University field experiments. *Water Resources Research* 17(3), 647–658.
USGS (2012). 3D Finite-difference groundwater flow model MODFLOW. *United States Geological Service*, http://water.usgs.gov/software/lists/groundwater.

Vandenbohede, A., Lebbe, L. (2011). Heat transport in a coastal groundwater flow system near De Panne, Belgium. *Hydrogeology Journal* 19, 1225–1238.

Voss, C., Provost, A.M. (2010). SUTRA, A model for saturated-unsaturated, variable-density ground-water flow with solute or energy transport. Version 2.2, Water Resources Investigations Report 02-4231, USGS Reston, Virginia, USA.

Werner, D., Kley, W. (1977). Problems of heat storage in aquifers. *Journal of Hydrology* 34, 35–43.

Wiberg, N.-E. (1983). Heat storage in aquifers analyzed by the finite element method. *Ground Water* 21(2), 178–187.

Woods, K., Ortega, A. (2011). The thermal response of an infinite line of open-loop wells for ground coupled heat pump systems. *International Journal of Heat and Mass Transfer* 54, 5574–5587.

Wu, Y.S., Ahlers, C.F., Fraser, P., Simmons, A., Pruess, K. (1996). Software qualification of selected TOUGH2 modules. Rep. LBNL-39490, Lawrence Berkeley National Laboratory Berkeley, California.

Xue, Y., Xie, C., Li, Q. (1990). Aquifer thermal energy storage: A numerical simulation of filed experiments in China. *Water Resources Research* 26(10), 2365–2375.

Yeh, G.-T., Luxmoore, R.J. (1983). Modeling moisture and thermal transport in unsaturated porous media. *Journal of Hydrology* 64, 299–309.

Zheng, C. (1990). MT3D, A modular three-dimensional transport model for simulation of advection, dispersion, and chemical reactions of contaminants in groundwater systems. Report to the Kerr Environmental Research Laboratory, US Environmental Protection Agency, Ada, Oklahoma.

Zheng, C., Wang, P.P. (1999). MT3DMS: A modular three dimensional multi-species transport model for simulation of advection, dispersion and chemical reactions of contaminants in groundwater systems; Documentation and user's guide. U.S. Army Engineer Research and Development Center Contract Report SERDP-99-1, Vicksburg, Mississippi.